

On the collision of two projectiles on two targets in the BFKL approach

M.A.Braun

Dep. of High Energy physics, Saint-Petersburg State University,
198504 S.Petersburg, Russia

August 21, 2021

Abstract

High-energy collisions of two nucleons on two nucleons are studied in the BFKL approach in the leading approximation in $\alpha_s N_c$. Diagrams with redistribution of colour are considered. It is found that intermediate BKP states consisting of 4 reggeized gluons give a contribution which may be leading in deuteron-deuteron scattering and thus experimentally observable.

1 Introduction

Collisions of two heavy nuclei have long occupied a prominent part of the experimental and theoretical studies in strong interactions at high energies. Unlike the case of DIS theoretical analysis of these processes turned out to be quite complicated. The most advanced calculations have been made in the framework of the Colour Glass Condensate approach, where they heavily rely on numerical Monte-Carlo method on the lattice to study evolution of the classical gluonic field in the course of collisions [1, 2, 3]. In comparison, analytic methods applied to collision of heavy nuclei have only given modest and approximate results [4, 5, 6]. So to understand the problem it seems natural to start not from this general case, but from the simplest generalization of the well-know results for DIS to the collision of two nucleons with two nucleons. The immediate physical application is of course the case of deuteron-deuteron collisions. An alternative view is to consider this as a particular contribution to the amplitude for the collision of two heavy nuclei A and B, which generally contains contributions from collisions of any number of nucleons in the projectile nucleus on any number of nucleons in the target. For large atomic numbers A and B the scattering amplitude is effectively unitarized by eikonalization of its connected part $E(b)$ of the corresponding diagrams:

$$\mathcal{A}_{AB} = 2is \int d^2b (1 - e^{-E(b)}), \quad (1)$$

where b is the impact parameter of the collision and s is the c.m energy squared for a pair of colliding nucleons. Our study then refers to the part of the eikonal function coming from the collision of two nucleons from the projectile nucleus on two nucleons from the target nucleus. Due to eikonalization the total nucleus-nucleus cross-section for heavy nuclei does not practically depend on a concrete value of the eikonal function. The latter is then large and its changes even by several times do not mean much for the total cross-section, which remains essentially geometrical. However even for heavy nuclei it may have influence on some specific processes, like exclusive rare production, where it may change the absorptive factor, and of course on the inclusive cross-sections.

It is instructive to see relative orders of magnitude for various contributions to the eikonal function $E(b)$. Naturally the leading order in both coupling constant α_s and number of colours N_c is given by the double gluon exchange, Fig. 1 *a*. For simplicity, instead of nucleons we shall consider quarks as elementary scattering centers in the nuclei, invoking the colour neutrality by projecting onto the colourless t -channels.

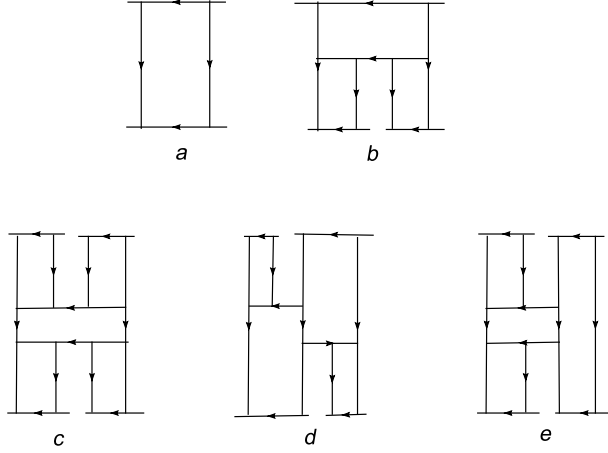


Figure 1: Lowest order diagrams for the eikonal: two gluon exchange (a) and with transitions to 2 (b) or 3 (c,d) intermediate gluons

Note that the total diagram for 2 by 2 scattering involves also the product of two such diagrams. However the eikonal function will include only one of them. If we forget about couplings inside the scattering centers, its contribution does not depend on α_s and is proportional to N_c^2 . Other connected diagrams may be classified by the minimal number of exchanged gluons n_{min} . We shall discuss their order of magnitude related to the double gluon exchange, Fig. 1 a. The diagram in Fig. 1 b with $n_{min} = 2$ has this relative order $\alpha_s^2 N_c^2$. The diagram in Fig. 1, c with $n_{min} = 2$ has the relative order $\alpha_s^4 N_c^4$. Diagrams d and e with $n_{min} = 3$ have order $\alpha_s^3 N_c^3$. Finally typical diagrams with $n_{min} = 4$ and redistribution of colour, which makes them connected, are shown in Fig. 2 and have the same order as Fig. 1a, so that their relative order is unity. To finally estimate the weights of these diagrams one has to take into account that diagrams with $n_{min} = 2$ and 3 involve one or two intermediate rapidities at which the initial and final 4 gluons fuse into the intermediate ones and so are proportional to y or y^2 where y is the overall rapidity. So their final order will be $\alpha_s^2 N_c^2 y$, $\alpha_s^4 N_c^4 y^2$ and $\alpha_s^3 N_c^3 y^2$. In the BFKL kinematics one assumes $\alpha_s N_c y \sim 1$, $\alpha_s N_c \ll 1$ so that orders of diagrams Fig. 1b, c, d and e become $\alpha_s N_c$, $\alpha_s^2 N_c^2$ and $\alpha_s N_c$ respectively. This shows that apart from the double gluon exchange the dominant contribution comes from the diagrams with colour redistribution, Fig. 2. Of course this result has been obtained in the lowest order, but it remains valid also in higher orders when the leading order will be multiplied by powers of $\alpha_s N_c y \sim 1$.

In this study we shall consider the connected part of the forward scattering amplitude of two projectile centers (quarks) on two target centers (also quarks). As we have demonstrated, in the lowest order it is just the simple rearrangement amplitude shown in Fig. 2 in two different forms: one (a) symmetric in projectiles and targets and another (b) showing the intermediate states in the s -channel. In fact both in Fig. 2 a and b one should also take into account all diagrams with crossed vertical lines (16 diagrams in all). We would like to study all possible inclusions of interactions between the gluons. They are realized by the BFKL interactions V_{ij} between gluon i and j [7]. We shall work in the leading approximation in the number of colours N_c . As compared to the disconnected diagram with two pomeron exchanges of the leading order in N_c , all contributions studied in the following will be of the order $1/N_c^2$ and so subdominant in the large N_c limit. However in the eikonal function they will contain an extra nuclear factor of the relative order $A^{2/3}$ for collisions of two nuclei of the same atomic number A and so in fact may be of the same order or even greater than the leading contribution in N_c .

We can separate all contributions into three classes. First, interactions may occur only between gluons attached to the same projectile or target and so being in the vacuum state. Such interactions will convert pairs of gluons attached to the projectiles and targets in Fig. 2 together with their crossing into fully developed pomeron Green functions, so that the quarks representing our projectiles

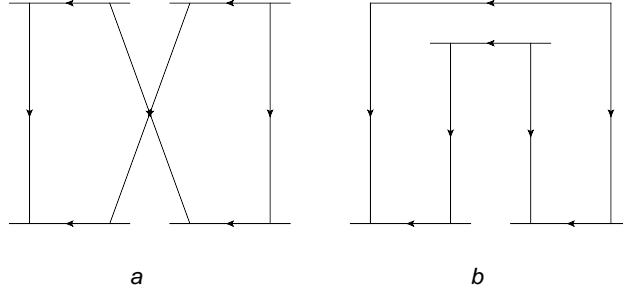


Figure 2: Lowest order diagram with a redistribution of color (diagrams with crossing gluon lines should be added)

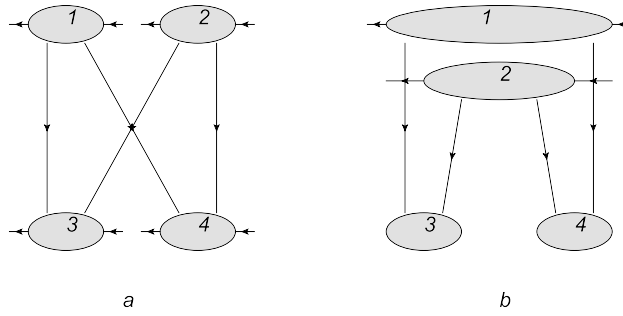


Figure 3: Diagrams for the direct transition of pomerons with the redistribution of colour

and targets will convert to pomerons, see Fig. 3. For heavy nuclei reggeized gluon splitting will further convert simple pomerons into fan diagrams made of pomerons, which are summed into the solution of the Balitski-Kovchegov (BK) equation, BK wave functions [8, 9].

Second class of the diagrams are formed from those of the first class with one interaction between the gluons V_{23} or V_{14} , which does not connect any pair of gluons in the vacuum state (Fig. 4).

Third class of the diagrams are those where from each side there appear interactions which connect vacuum pairs of gluons with the so-called BKP states [10, 11] between them. (Fig. 5).

Before actually calculating all these contributions, in Section 2 we develop a multirapidity formalism which makes it easier to sew four pomerons into a single amplitude.

Let the momenta of the nucleons in the projectile be k and those in the target be l . In the c.m.

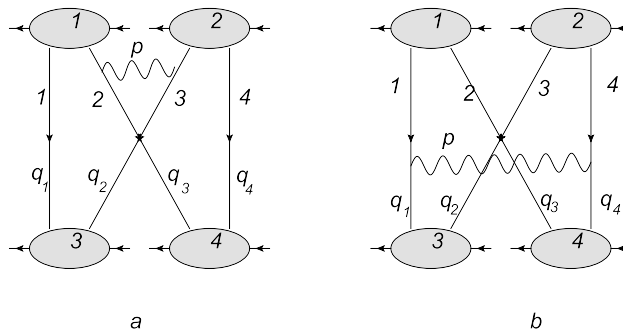


Figure 4: Diagrams with the redistribution of colour and one interaction between the pomerons of the projectile and target

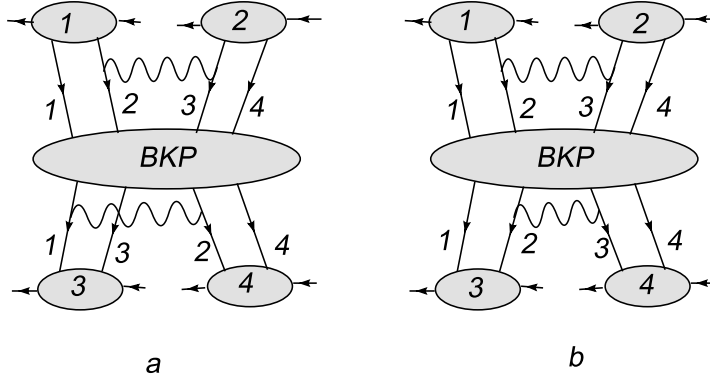


Figure 5: Diagrams with the intermediate BKP states

system of a pair of nucleons from the projectile and target we have

$$k_+ = l_-, \quad k_- = k_\perp = l_+ = l_\perp = 0, \quad s = 2k_+l_-$$

The amplitude for nucleus-nucleus scattering can be separated into its high-energy part H and two nuclear factors (see Appendix 1.). The imaginary part of H in its turn can be presented in the form

$$\text{Im } H = -(2\pi)^2 \delta(\kappa_+) \delta(q_-) 4s^2 N_c^2 D, \quad (2)$$

where κ and q are the momenta transferred into the projectile and target nuclei respectively with $\kappa_- = \kappa_\perp = q_+ = q_\perp = 0$ and D is a real function which is the sum of connected diagrams for the forward scattering of two-nucleons on two nucleons written as integrals in rapidity and transverse momentum space. At fixed impact parameter b the cross-section for the part of nucleus-nucleus scattering coming from interactions of two nucleons from the projectile on two nucleons from target is related to D as

$$\sigma_{AB}^{(2)}(b) = -2N_c^2 D \int d^2b_A T_A^2(b_A) T_B^2(b - b_A) \quad (3)$$

and for deuteron-deuteron scattering

$$\sigma_{dd} = -2N_c^2 D \left\langle \frac{1}{2\pi r^2} \right\rangle_d^2 \quad (4)$$

(see Appendix 1.).

Note in conclusion that the contribution of simplest diagrams with colour rearrangements have been considered in literature in relation to correlations between a pair of produced gluons [12]. We postpone discussion of the inclusive gluon production to future publications, since in our BFKL-Bartels approach it involves the study of possible cuts of the forward scattering amplitudes, which for 2 by 2 scattering requires special attention to the well-known AGK cancellations. Meanwhile we have to stress that already on the level of the total cross-section, apart from the pomeron (or BK) wave function, our amplitudes involve more complicated objects made of 4 reggeized gluons (the BKP states). In the Colour Glass Condensate approach similar complicated structures begin to appear only on the level of double inclusive cross-sections.

2 Pomeron in the multirapidity formalism

In this section we introduce a formalism in which each pomeron has its own rapidity, which corresponds to the standard Feynman diagram technique. In this formalism construction of amplitudes with colour rearrangement becomes much simpler. Recall that in the BFKL approach the amplitude ("wave function") $P(y)$ at a given rapidity y is obtained from its value at $y = 0$ by the transformation

$$P(y) = e^{-yH} P(0). \quad (5)$$

Here the BFKL Hamiltonian is $H = H^{(0)} + V$. The unperturbed Hamiltonian $H^{(0)}$ is a sum of Regge trajectories $\omega(k)$ with a minus sign. For gluons 1 and 2 $H_{12}^{(0)} = -\omega_1 - \omega_2$ or, in the momentum representation,

$$\langle k'_1, k'_2 | H^{(0)} | k_1, k_2 \rangle = -(2\pi)^4 \delta^2(k_1 - k'_1) \delta^2(k_2 - k'_2) (\omega(k_1) + \omega(k_2)). \quad (6)$$

The potential energy V is given by the pair BFKL interaction. Symmetrizing in initial and final reggeons we have

$$V_{12} = (T_1 T_2) (2\pi)^2 \delta^2(k_1 + k_2 - k'_1 - k'_2) v(k'_1, k'_2 | k_1, k_2), \quad (7)$$

where

$$v(k'_1, k'_2 | k_1, k_2) = \frac{g^2}{2\pi k_1 k_2 k'_1 k'_2} \left(\frac{k_1^2 k_2'^2 + k_2^2 k_1'^2}{(k_1 - k'_1)^2} - (k_1 + k_2)^2 \right) \quad (8)$$

and T_1 and T_2 are colours of the two gluons.

Evolution law (5) mimics the standard evolution in time provided one makes the substitution

$$t \rightarrow -iy, \quad y \rightarrow it, \quad y > 0. \quad (9)$$

By definition $P(y) = 0$ at $y < 0$. We shall obtain our diagrammatic technique studying evolution in time. Evolution in rapidity will be obtained making the analytic continuation (9) at $y > 0$ in final formulas.

Passing to the multirapidity formalism we shall additionally characterize each reggeon by its "energy" ϵ . We shall take the reggeon propagator as a function of ϵ in the form

$$\Delta(\epsilon, k) = \frac{i}{\epsilon + \omega(k) + i0}. \quad (10)$$

Then as a function of time

$$\Delta(t, k) = i \int \frac{d\epsilon}{2\pi} e^{-i\epsilon t} \frac{1}{\epsilon + \omega(k) + i0} = \theta(t) e^{it\omega(k)}. \quad (11)$$

Taking $it \rightarrow y$ at $t > 0$ and $y > 0$ we get the desired reggeon propagator

$$\Delta(y, k) = \theta(y) e^{y\omega(k)}. \quad (12)$$

The interaction between reggeons will be given by (7) with factor $(-i)$ and with an additional factor responsible for conservation of the total energy

$$\hat{V}_{12} = -i(T_1 T_2) (2\pi)^3 \delta(\epsilon_1 + \epsilon_2 - \epsilon'_1 - \epsilon'_2) \delta^2(k_1 + k_2 - k'_1 - k'_2) v(k'_1, k'_2 | k_1, k_2). \quad (13)$$

These Feynman rules allow to construct amplitudes for the interaction of any number of reggeons provided this number does not change.

Our first task is to check that for a pair of reggeons the sum of all thus constructed Feynman diagrams is equivalent to the standard BFKL equation.

The Green function for a pair of interacting reggeons $\mathcal{G}(\epsilon'_1 k'_1, \epsilon'_2 k'_2 | \epsilon_1 k_1, \epsilon_2 k_2)$, which is illustrated in Fig. 6, obeys an equation which is graphically shown in Fig. 7.

Separating from \mathcal{G} the δ -functions which corresponds to energy-momentum conservation

$$\mathcal{G}(\epsilon'_1 k'_1, \epsilon'_2 k'_2 | \epsilon_1 k_1, \epsilon_2 k_2) = (2\pi)^3 \delta(\epsilon'_1 + \epsilon'_2 - \epsilon_1 - \epsilon_2) \delta^2(k'_1 + k'_2 - k_1 - k_2) \mathcal{G}_{EK}(\epsilon'_1 k'_1 | \epsilon_1 k_1), \quad (14)$$

where $E = \epsilon_1 + \epsilon_2 = \epsilon'_1 + \epsilon'_2$ and $K = k_1 + k_2 = k'_1 + k'_2$. we find a Bethe-Salpeter type equation for \mathcal{G}_{EK}

$$\mathcal{G}_{EK}(\epsilon'_1 k'_1 | \epsilon_1 k_1) = (2\pi)^3 \delta(\epsilon'_1 - \epsilon_1) \delta^2(k'_1 - k_1) \Delta_1 \Delta_2 + \Delta'_1 \Delta'_2 \int \frac{d\epsilon''_1 d^2 k''_1}{(2\pi)^3} \hat{V}(k'_1, k'_2 | k''_1, k''_2) \mathcal{G}_{EK}(\epsilon''_1 k''_1 | \epsilon_1 k_1), \quad (15)$$

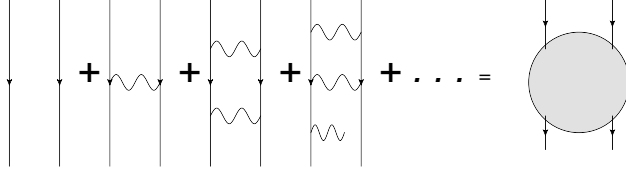


Figure 6: The pomeron Green function \mathcal{G}

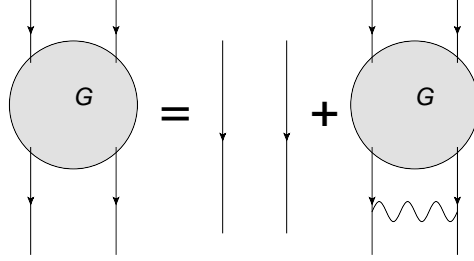


Figure 7: Equation for the pomeron Green function \mathcal{G}

where we denote $\Delta_1 = i/(\epsilon_1 + \omega_1)$, $\Delta'_1 = i/(\epsilon'_1 + \omega'_1)$ and so on and all ω 's are assumed to have a small positive imaginary part.

In this equation the interaction is energy independent, as in theories with non-relativistic potentials. So it can be easily transformed into a Schroedinger-like equation. Indeed if we present

$$\mathcal{G}_{EK}(\epsilon'_1 k'_1 | \epsilon_1 k_1) = (2\pi)^3 \delta(\epsilon'_1 - \epsilon_1) \delta^2(k'_1 - k_1) \Delta_1 \Delta_2 + \Delta'_1 \Delta'_2 \hat{T}_{EK} \Delta_1 \Delta_2 \quad (16)$$

then $\hat{T}_{EK}(\epsilon'_1 k'_1 | \epsilon_1 k_1)$ does not depend on initial nor final energies ϵ_1 , ϵ_2 , ϵ'_1 and ϵ'_2 . The equation for \hat{T} takes the form

$$\hat{T}_{EK}(k'_1 | k_1) = \hat{V}(k'_1, k'_2 | k_1, k_2) + \int i \frac{d^2 k''_1}{(2\pi)^2} \frac{\hat{V}(k'_1, k'_2 | k''_1, k''_2) \hat{T}_{EK}(k''_1 | k_1)}{E + \omega''_1 + \omega''_2 + i0} \quad (17)$$

Recalling that $\hat{V} = -iV$, where $V = (T_1 T_2)v$, and putting $\hat{T} = -iT$ we rewrite Eq. (17) in the operatorial form

$$T_{EK} = V + V R_{EK} T_{EK} \quad (18)$$

where

$$R_{EK} = (E - H^{(0)} + i0)^{-1} \quad (19)$$

is the resolvent of the unperturbed Hamiltonian. Eq. (18) is the standard equation for the T -matrix. The standard BFKL Green function is defined by T_{EK} as

$$G_{EK} = R_{EK} + R_{EK} T_{EK} R_{EK} = (E - H)^{-1} \quad (20)$$

The Bethe-Salpeter Green function \mathcal{G} is expressed via the Schroedinger one G , as

$$\begin{aligned} \mathcal{G}_{EK}(\epsilon'_1 k'_1 | \epsilon_1 k_1) &= (2\pi)^3 \delta(\epsilon'_1 - \epsilon_1) \delta^2(k'_1 - k_1) \Delta_1 \Delta_2 + i(2\pi)^2 \delta^2(k'_1 - k_1) [E + \omega_1 + \omega_2] \Delta'_1 \Delta'_2 \Delta_1 \Delta_2 \\ &\quad - i \Delta'_1 \Delta'_2 [E + \omega'_1 + \omega'_2] G_{EK}(k'_1 | k_1) [E + \omega_1 + \omega_2] \Delta_1 \Delta_2. \end{aligned} \quad (21)$$

Now we pass to the BFKL function proper. Integrating the Green function $\mathcal{G}_{EK}(\epsilon'_1 k'_1 | \epsilon_1 k_1)$ with the impact factor $\rho_{EK}(k'_1)/(k'_1 k'_2)$ we obtain a function which describes the pomeron in the multirapidity formalism

$$\mathcal{P}_{EK}(\epsilon_1 k_1) = \int \frac{d\epsilon'_1 d^2 k'_1}{(2\pi)^3 k'_1 k'_2} \rho_{EK}(k'_1) \mathcal{G}_{EK}(\epsilon'_1 k'_1 | \epsilon_1 k_1). \quad (22)$$

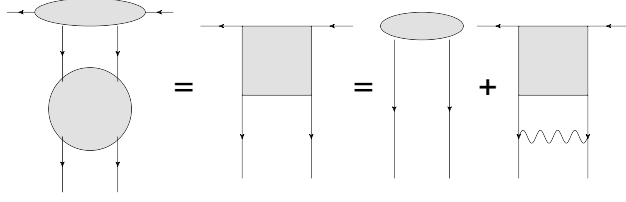


Figure 8: Equation for the pomeron wave function \mathcal{P}

The equation for it easily follows from Fig. 8

$$\mathcal{P}_{EK}(\epsilon_1 k_1) = \mathcal{P}_{EK}^{(0)}(\epsilon_1 k_1) - i\Delta_1 \Delta_2 \int \frac{d\epsilon'_1 d^2 k'_1}{(2\pi)^3} V(k_1, k_2 | k'_1, k'_2) \mathcal{P}_{EK}(\epsilon'_1 k'_1), \quad (23)$$

where $\epsilon_2 = E - \epsilon_1$, $k_2 = K - k_1$ and $\omega_2 = \omega(k_2)$. If we introduce the "amputated" wave function by

$$\mathcal{P}_{EK}(\epsilon_1 k_1) = F_{EK}(\epsilon_1, k_1) \Delta_1 \Delta_2 \quad (24)$$

then F does not depend on energy ϵ_1 and satisfies

$$F_{EK}(k_1) = F_{EK}^{(0)}(k_1) + \int \frac{d^2 k'_1}{(2\pi)^2} \frac{V(k_1, k_2 | k'_1, k'_2) F_{EK}(\epsilon'_1 k'_1)}{E + \omega'_1 + \omega'_2}. \quad (25)$$

So if we define a new wave function

$$P_{EK}(k_1) = \frac{F_{EK}(k_1)}{E + \omega_1 + \omega_2} \quad (26)$$

it will obey the equation

$$(E + \omega_1 + \omega_2) P_{EK}(k_1) = F_{EK}^{(0)}(k_1) + \int \frac{d^2 k'_1}{(2\pi)^2} V(k_1, k_2 | k'_1, k'_2) P_{EK}(k'_1), \quad (27)$$

which is the standard BFKL equation (for the pomeron or gluon depending on the value of $(T_1 T_2)$ in V).

Note that BS function \mathcal{P} turns out to be related to P as

$$\mathcal{P}_{EK}(\epsilon_1 k_1) = \frac{E + \omega_1 + \omega_2}{(\epsilon_1 + \omega_1)(\epsilon_2 + \omega_2)} P_{EK}(k_1). \quad (28)$$

It depends on the individual energies. It is remarkable that although for the pomeron P is infrared safe, the corresponding BS function \mathcal{P} does not look so.

3 Four pomerons sewed with the redistribution of colour

Now we pass to the simplest amplitude D_1 in which two pomerons from the projectile (reggeon pairs (1,2) and (3,4)) are directly coupled to two pomerons in the target (reggeon pairs (13) and (24)) illustrated in Fig. 3. All pomerons will have their total momenta equal to zero, which will be tacitly assumed in the following. The pomerons from the projectile have their total energies E_{12} and E_{34} and those from the target energies E_{13} and E_{24} . Energy conservation requires $E_{12} + E_{34} = E_{13} + E_{24}$. Correspondingly the amplitude $D_1(E_{12}, E_{34}, E_{13}, E_{24})$ will include factor $2\pi\delta(E_{12} + E_{34} - E_{13} - E_{24})$ which will be suppressed in the following. As seen from Fig. 3, the internal integrations will include a single transverse momentum q and a single pomeron energy, say, ϵ_1 . The remaining energies will be expressed via ϵ_1 as follows

$$\epsilon_2 = E_{12} - \epsilon_1, \quad \epsilon_3 = E_{13} - \epsilon_1, \quad \epsilon_4 = E_{24} - \epsilon_2 = E_{24} - E_{12} + \epsilon_1. \quad (29)$$

In terms of the amputated pomeron function F the amplitude will be given by

$$D_1(E_{12}, E_{34}, E_{13}, E_{24}) = \int \frac{d\epsilon_1 d^2 q}{(2\pi)^3} \frac{F_{E_{12}}(q) F_{E_{34}}(q) F_{E_{13}}(q) F_{E_{24}}(q)}{(\epsilon_1 + \omega(q))(\epsilon_2 + \omega(q))(\epsilon_3 + \omega(q))(\epsilon_4 + \omega(q))}, \quad (30)$$

where all ω 's are assumed to have a small positive imaginary part.

Since F 's do not depend on ϵ_1 we can do integration on ϵ_1 explicitly. We have an integral

$$\begin{aligned} I &= \int \frac{d\epsilon_1}{2\pi} \frac{1}{\epsilon_1 + \omega(q) + i0} \frac{1}{E_{12} - \epsilon_1 + \omega(q) + i0} \frac{1}{E_{13} - \epsilon_1 + \omega(q) + i0} \frac{1}{E_{24} - E_{12} + \epsilon_1 + \omega(q) + i0} \\ &= -\frac{i}{E_{13} - E_{12}} \left\{ \frac{1}{E_{12} + 2\omega(q) + i0} \frac{1}{E_{24} + 2\omega(q) + i0} - \frac{1}{E_{13} + 2\omega(q) + i0} \frac{1}{E_{34} + 2\omega(q) + i0} \right\}. \end{aligned} \quad (31)$$

Now we express our amputated pomerons F via full ones P using Eq. (26). In terms of P the amplitude will be given by

$$D_1(E_{12}, E_{34}, E_{13}, E_{24}) = -i \int \frac{d^2 q}{(2\pi)^2} (E_{12} + E_{34} + 4\omega(q)) P_{E_{12}}(q) P_{E_{34}}(q) P_{E_{13}}(q) P_{E_{24}}(q). \quad (32)$$

Immediately the question of its infrared safeness arises, since the integrand contains the reggeon trajectory $\omega(q)$.

Next we study evolution in rapidity.

$$\begin{aligned} D_1(y) &= \int \frac{dE_{12} dE_{34} dE_{13} dE_{24}}{(2\pi)^4} 2\pi \delta(E_{12} + E_{34} - E_{13} - E_{24}) e^{-y(E_{12} + E_{34})} D_1(E_{12}, E_{34}, E_{13}, E_{24} = \\ &\quad -i \int \frac{d^2 q}{(2\pi)^2} \left(4\omega(q) - \frac{\partial}{\partial y} \right) \int \frac{dE_{12} dE_{34} dE_{13} dE_{24}}{(2\pi)^4} 2\pi \delta(E_{12} + E_{34} - E_{13} - E_{24}) \\ &\quad e^{-y(E_{12} + E_{34})} P_{E_{12}}(q) P_{E_{34}}(q) P_{E_{13}}(q) P_{E_{24}}(q). \end{aligned} \quad (33)$$

We first consider evolution of the integrand of the momentum integral in time:

$$\begin{aligned} Z(t) &= \int \frac{dE_{12} dE_{34} dE_{13} dE_{24}}{(2\pi)^4} 2\pi \delta(E_{12} + E_{34} - E_{13} - E_{24}) e^{-it(E_{12} + E_{34})} P_{E_{12}}(q) P_{E_{34}}(q) P_{E_{13}}(q) P_{E_{24}}(q) \\ &= \int \frac{dE_{12} dE_{34} dE_{13} dE_{24}}{(2\pi)^4} d\tau e^{i\tau(E_{12} + E_{34} - E_{13} - E_{24})} e^{-it(E_{12} + E_{34})} P_{E_{12}}(q) P_{E_{34}}(q) P_{E_{13}}(q) P_{E_{24}}(q). \end{aligned} \quad (34)$$

We use

$$\int dE P_E(q) e^{-itE} = \theta(t) P(t, q) \quad (35)$$

to obtain

$$Z(t) = \int d\tau \theta(t - \tau) P^2(t - \tau, q) \theta(\tau) P^2(\tau, q) = \theta(t) \int_0^t d\tau P^2(t - \tau, q) P^2(\tau, q). \quad (36)$$

Analytic continuation to rapidity gives

$$Z(y) = -i \int dy' \theta(y - y') P^2(y - y', q) \theta(y') P^2(y', q) = -i \theta(y) \int_0^y dy' P^2(y - y', q) P^2(y', q), \quad (37)$$

so that finally

$$D_1(y) = -\theta(y) \int \frac{d^2 q}{(2\pi)^2} \left(4\omega(q) - \frac{\partial}{\partial y} \right) \int_0^y dy' P^2(y - y', q) P^2(y', q). \quad (38)$$

To check the correctness of the transition from time to rapidity we study a simple model, in which P_E is given by a BFKL pole

$$P_E = \frac{1}{E + a + i0}, \quad (39)$$

so that $P(y) = \theta(y)e^{ay}$. In this case it is easy to find evolution of $Z(y)$ in rapidity by explicit analytic continuation. Let for complex z

$$Z(z) = \int \frac{dE dE_{12} dE_{13}}{(2\pi)^3} e^{-zE} P_{E_{12}}(q) P_{E-E_{12}}(q) P_{E_{13}}(q) P_{E-E_{13}}(q). \quad (40)$$

We have

$$\int \frac{dE'}{2\pi} P_{E'} P_{E-E'} = \int \frac{dE'}{2\pi} \frac{1}{(E' + a + i0)(E - E' + a + i0)} = -i \frac{1}{E + 2a + i0}.$$

So we find

$$Z(z) = - \int \frac{dE}{2\pi} e^{-zE} \frac{1}{(E + 2a + i0)^2} = i \frac{\partial}{\partial E} e^{-zE} \big|_{E=-2a} = -ize^{2az}. \quad (41)$$

But this integral only exists for pure imaginary $z = it$ when it is given

$$Z(t) = - \int \frac{dE}{2\pi} e^{-itE} \frac{1}{(E + 2a + i0)^2} = +i\theta(t) \frac{\partial}{\partial E} e^{-itE} \big|_{E=-2a} = te^{2ait} \rightarrow -ize^{2az}. \quad (42)$$

On the other hand, from (37) we find

$$Z(y) = -i\theta(y) \int_0^y dy' e^{2a(y-y')} e^{2ay'} = -iy e^{2ay} \quad (43)$$

in accordance with (41). This confirms factor $(-i)$ in (37) and so (38).

4 Single interaction between the projectile and target pomerons

Now we consider diagrams with a single interaction between the projectile and target which cannot be included into the pomerons, that is V_{23} or V_{14} , see Figs. 4a and b.

We start with the diagram shown in Fig. 4a. As before we suppress the energy conservation factor $2\pi\delta(E_{12} + E_{34} - E_{13} - E_{24})$. The diagram contains two loops and so integrations over $\epsilon_1, \epsilon_4, q_1$ and q_4 . Energy-momenta of the gluons 1,2,3 and 4 before the interaction are

$$(\epsilon_1, q_1), (E_{12} - \epsilon_1, -q_1), (E_{34} - \epsilon_4, -q_4), (\epsilon_4, q_4). \quad (44)$$

After the interaction gluon 2 and 3 have their energy-momenta $(E_{24} - \epsilon_4)$ and $(E_{31} - \epsilon_1, -q_1)$ respectively. In terms of amputated pomerons F the contribution from Fig. 4 a is

$$D_{2a} = i \int \frac{d\epsilon_1 d\epsilon_4 d^2 q_1 d^2 q_4 F_{E_{12}}(q_1) F_{E_{34}}(q_4) F_{E_{13}}(q_1) F_{E_{24}}(q_4) V(-q_1, -q_4 | -q_4, -q_1)}{(2\pi)^6 (\epsilon_1 + \omega_1)(E_{12} - \epsilon_1 + \omega_1)(E_{13} - \epsilon_1 + \omega_1)(\epsilon_4 + \omega_4)(E_{34} - \epsilon_4 + \omega_4)(E_{24} - \epsilon_4 + \omega_4)}. \quad (45)$$

The prefactor includes $-i$ from the definition of \hat{V} and (-1) from 6 propagators.

Integration over energies factorizes into two integrals:

$$I_1 = \int \frac{d\epsilon_1}{2\pi(\epsilon_1 + \omega_1 + i0)(E_{12} - \epsilon_1 + \omega_1 + i0)(E_{13} - \epsilon_1 + \omega_1 + i0)} = -i \frac{1}{(E_{12} + 2\omega_1)(E_{13} + 2\omega_1)} \quad (46)$$

and a similar integral over ϵ_4 which gives

$$I_2 = -i \frac{1}{(E_{34} + 2\omega_4)(E_{24} + 2\omega_4)}. \quad (47)$$

So we get

$$D_{2a} = -i \int \frac{d^2 q_1 d^2 q_4 F_{E_{12}}(q_1) F_{E_{34}}(q_4) F_{E_{13}}(q_1) F_{E_{24}}(q_4) V(-q_1, -q_4 | -q_4, -q_1)}{(2\pi)^4 (E_{12} + 2\omega_1)(E_{13} + 2\omega_1)(E_{34} + 2\omega_4)(E_{24} + 2\omega_4)}. \quad (48)$$

Recalling relation (26) between the amputated wave function F and pomeron we rewrite this as

$$D_{2a} = -i \int \frac{d^2 q_1 d^2 q_4}{(2\pi)^4} P_{E_{12}}(q_1) P_{E_{34}}(q_4) P_{E_{13}}(q_1) P_{E_{24}}(q_4) V(-q_1, -q_4 | -q_4, -q_1). \quad (49)$$

Now we pass to the amplitude corresponding to the diagram in Fig. 4 b. Before the interaction gluons 1,2,3 and 4 have the same energy-momenta as before (Eq(44)). However now the momenta of gluons 1 and 4 change after the interaction and become $(E_{13} - E_{34} + \epsilon_4, q_4)$ and $(E_{24} - E_{12} + \epsilon_1)$ respectively.

In terms of F the amplitude is

$$D_{2b} = i \frac{1}{(2\pi)^6} \times \int \frac{d\epsilon_1 d\epsilon_4 d^2 q_1 d^2 q_4 F_{E_{12}}(q_1) F_{E_{34}}(q_4) F_{E_{13}}(q_4) F_{E_{24}}(q_1) V(q_1, q_4 | q_4, q_1)}{(\epsilon_1 + \omega_1)(E_{12} - \epsilon_1 + \omega_1)(E_{24} - E_{12} + \epsilon_1 + \omega_1)(\epsilon_4 + \omega_4)(E_{34} - \epsilon_4 + \omega_4)(E_{13} - E_{34} + \epsilon_4 + \omega_4)}. \quad (50)$$

Again the integrals over energies factorize into two ones:

$$I_3 = \int \frac{d\epsilon_1}{2\pi(\epsilon_1 + \omega_1 + i0)(E_{12} - \epsilon_1 + \omega_1 + i0)(E_{24} - E_{12} + \epsilon_1 + \omega_1 + i0)} = i \frac{1}{(E_{12} + 2\omega_1)(E_{24} + 2\omega_1)} \quad (51)$$

and a similar integral over ϵ_4

$$I_4 = i \frac{1}{(E_{34} + 2\omega_4)(E_{13} + 2\omega_4)}. \quad (52)$$

We get

$$D_{2b} = -i \int \frac{d^2 q_1 d^2 q_4 F_{E_{12}}(q_1) F_{E_{34}}(q_4) F_{E_{13}}(q_4) F_{E_{24}}(q_1) V(q_1, q_4 | q_4, q_1)}{(2\pi)^4 (E_{12} + 2\omega_1)(E_{13} + 2\omega_4)(E_{34} + 2\omega_4)(E_{24} + 2\omega_1)} \quad (53)$$

or in terms of pomerons P

$$D_{2b} = -i \int \frac{d^2 q_1 d^2 q_4}{(2\pi)^4} P_{E_{12}}(q_1) P_{E_{34}}(q_4) P_{E_{13}}(q_4) P_{E_{24}}(q_1) V(q_1, q_4 | q_4, q_1). \quad (54)$$

Let us separate the infrared stable and divergent parts in D_2 . For a pair of gluons 1 and 2 the BFKL Hamiltonian is

$$H = -\omega_1 - \omega_2 + (T_1 T_2) v_{12},$$

where v_{12} is given by (8). In the vacuum t -channel $(T_1 T_2) = -N_c$, so that the infrared stable pomeron Hamiltonian is

$$H_P = -\omega_1 - \omega_2 - N_c v_{12}. \quad (55)$$

In D_2 interaction connects different colour configurations with gluons from the projectile forming colourless pairs (1,2) and (3,4) and from the target forming colorless pairs (1,3) and (2,4). The transition matrix element of $(T_2 T_3)$ entering the interaction is $+N_c$ (see Appendix 2.). So in terms of v amplitude D_{2a} is given by

$$D_{2a} = -i \int \frac{d^2 q_1 d^2 q_4}{(2\pi)^4} P_{E_{12}}(q_1) P_{E_{34}}(q_4) P_{E_{13}}(q_1) P_{E_{24}}(q_4) N_c v(-q_1, -q_4 | -q_4, -q_1). \quad (56)$$

We present

$$N_c v(-q_1, -q_4 | -q_4, -q_1) = - \langle -q_1, -q_4 | H_P | -q_4, -q_1 \rangle - 2\omega_1 (2\pi)^2 \delta^2(q_1 - q_4), \quad (57)$$

so that

$$D_{2a} = i \int \frac{d^2 q_1 d^2 q_4}{(2\pi)^4} P_{E_{12}}(q_1) P_{E_{34}}(q_4) P_{E_{13}}(q_1) P_{E_{24}}(q_4) \langle -q_1, -q_4 | H_P | -q_4, -q_1 \rangle$$

$$+ 2i \int \frac{d^2 q}{(2\pi)^2} \omega(q) P_{E_{12}}(q) P_{E_{34}}(q) P_{E_{13}}(q) P_{E_{24}}(q) \quad (58)$$

and similarly

$$D_{2b} = i \int \frac{d^2 q_1 d^2 q_4}{(2\pi)^4} P_{E_{12}}(q_1) P_{E_{34}}(q_4) P_{E_{13}}(q_4) P_{E_{24}}(q_1) < q_1, q_4 | H_P | q_4, q_1 > \\ + 2i \int \frac{d^2 q}{(2\pi)^2} \omega(q) P_{E_{12}}(q) P_{E_{34}}(q) P_{E_{13}}(q) P_{E_{24}}(q). \quad (59)$$

As we see the additional terms in (58) and (59) containing $\omega(q)$ cancel with a similar term in (32), so that the remaining sum of D_1 and D_2 turns out to be infrared safe.

So after cancellation of the gluon Regge trajectories the infrared safe contributions from diagrams in Figs. 3 and 4 are

$$D_1 = \theta(y) \frac{\partial}{\partial y} \int_0^y dy' \int \frac{d^2 q}{(2\pi)^2} P^2(y - y', q) P^2(y', q) \quad (60)$$

and

$$D_2 = 2\theta(y) \int_0^y dy' \int \frac{d^2 q d^2 q'}{(2\pi)^4} < q, q' | H | q', q > P(y - y', q) P(y - y', q') P(y', q) P(y', q'). \quad (61)$$

5 Two interactions between the projectile and target pomerons

With two interactions between the target and projectile pomerons we can use our old results in [13] where coupling of two pomerons to the BKP 4-gluon case was studied (see also Appendix 2.)

In this case there are transitions both with the redistribution of colour, that is $|(12)(34) \rightarrow (13)(24) \rangle$, and without this redistribution, that is $|(12)(34) \rightarrow (12)(34) \rangle$.

To continue our line of studies we start with the redistribution of colour. As follows from our studies in Appendix 2 in this case between the pomerons from the projectile and target there can appear two 4-gluon BKP states $|1243 \rangle$ and $|1324 \rangle$. Inserting the 4-gluon BKP Green function G between them we find that the projectile and target pomerons will be connected by

$$M_E^{(a)} = \frac{1}{4} N_c^2 (v_{13} + v_{24} - v_{23} - v_{14}) [G_E^{(1243)} + G_E^{(1342)}] (v_{12} + v_{34} - v_{23} - v_{14}), \quad (62)$$

where, say, $G_E^{(1243)}$ is an operator acting in the 4-gluon space

$$< q_1, q_2, q_3, q_4 | G_E^{(1243)} | q'_1, q'_2, q'_3, q'_4 >$$

satisfying the equation

$$(E - H^{(1243)}) G_E^{1243} = 1 \quad (63)$$

with

$$H^{(1243)} = - \sum_{i=1}^4 \omega_i - \frac{1}{2} g^2 N_c (v_{12} + v_{24} + v_{43} + v_{31}). \quad (64)$$

Note that $M_E^{(a)}$ can also be presented in terms of the infrared safe BFKL Hamiltonian for the pomeron H_P

$$M_E^{(a)} = \frac{1}{4} (H_{P,13} + H_{P,24} - H_{P,23} - H_{P,14}) [G_E^{(1243)} + G_E^{(1324)}] (H_{P,12} + H_{P,34} - H_{P,23} - H_{P,14}) \quad (65)$$

which demonstrates that $M_E^{(a)}$ is infrared safe.

The explicit form for the kernel of M is

$$< q_1, q_2, q_3, q_4 | M_E^{(a)} | q'_1, q'_2, q'_3, q'_4 > = 2\pi\delta^2 \left(\sum_{j=1}^4 q'_j - \sum_{j=1}^4 q_j \right) \frac{1}{4} N_c^2 \int \prod_{j=1}^4 \frac{d^2 k'_j}{(2\pi)^2} \frac{d^2 k_j}{(2\pi)^2} 2\pi\delta^2 \left(\sum_{j=1}^4 k'_j - \sum_{j=1}^4 k_j \right)$$

$$\begin{aligned}
& < q_1, q_2, q_3, q_4 | v_{13} + v_{24} - v_{23} - v_{14} | k_1, k_2, k_3, k_4 > < k_1, k_2, k_3, k_4 | G_E^{(1243)} + G_E^{(1342)} | k'_1, k'_2, k'_3, k'_4 > \\
& < k'_1, k'_2, k'_3, k'_4 | v_{12} + v_{34} - v_{23} - v_{14} | q'_1, q'_2, q'_3, q'_4 >, \tag{66}
\end{aligned}$$

where for instance

$$< q_1, q_2, q_3, q_4 | v_{13} | k_1, k_2, k_3, k_4 > = (2\pi)^4 \delta^2(q_2 - k_2) \delta^2(q_4 - k_4) v(q_1, q_3 | k_1, k_3) \tag{67}$$

and $v(q_1, q_3 | k_1, k_3)$ is given by (8).

The amplitude D_3 with the redistribution of colour corresponding to Fig. 5 will be given by

$$\begin{aligned}
D_{3a} &= - \int \frac{dE_1}{2\pi} \frac{dE'_1}{2\pi} \int \prod_{j=1}^4 \frac{d^2 q'_j}{(2\pi)^2} \frac{d^2 q_j}{(2\pi)^2} 2\pi \delta^2 \left(\sum_{j=1}^4 q'_j - \sum_{j=1}^4 q_j \right) \\
P_{E-E_1}(q_1) P_{E_1}(q_4) &< q_1, -q_1, -q_4, q_4 | M_E^{(a)} | q'_1, -q'_1, -q'_4, q'_4 > P_{E-E'_1}(q'_1) P_{E'_1}(q'_4). \tag{68}
\end{aligned}$$

The prefactor includes two $(-i)$ from \hat{V} .

The amplitude without colour redistribution will differ from D_{3a} in that between the projectile and target pomerons now appear four BKP states $|1234\rangle$, $|1243\rangle$, $|1342\rangle$ and $|1432\rangle$ and their coupling to the projectile and target pomerons will be the same. This means that now the projectile and target pomerons will be connected by

$$\begin{aligned}
M_E^{(b)} &= \frac{1}{4} N_c^2 (v_{13} + v_{24} - v_{23} - v_{14}) [G_E^{(1234)} + G_E^{(1432)} + G_E^{(1243)} + G_E^{(1342)}] (v_{13} + v_{24} - v_{23} - v_{14}) \\
&= \frac{1}{4} (H_{P,13} + H_{P,24} - H_{P,23} - H_{P,14}) [G_E^{(1234)} + G_E^{(1432)} + G_E^{(1243)} + G_E^{(1342)}] \\
&\quad (H_{P,13} + H_{P,24} - H_{P,23} - H_{P,14}). \tag{69}
\end{aligned}$$

The remaining formulas do not change and we find that the amplitude D_{3b} without colour redistribution corresponding to Fig. 5 will be given by

$$\begin{aligned}
D_{3b} &= - \int \frac{dE_1}{2\pi} \frac{dE'_1}{2\pi} \int \prod_{j=1}^4 \frac{d^2 q'_j}{(2\pi)^2} \frac{d^2 q_j}{(2\pi)^2} 2\pi \delta^2 \left(\sum_{j=1}^4 q'_j - \sum_{j=1}^4 q_j \right) \\
P_{E-E_1}(q_1) P_{E_1}(q_4) &< q_1, -q_1, -q_4, q_4 | M_E^{(b)} | q'_1, -q'_1, -q'_4, q'_4 > P_{E-E'_1}(q'_1) P_{E'_1}(q'_4). \tag{70}
\end{aligned}$$

To pass to rapidity, consider first evolution of the momentum integrand in time.

$$Z_1 = \int \frac{dE dE_1 dE_2}{(2\pi)^3} e^{-iEt} P_{E-E_1} P_{E_1} P_{E-E_2} P_{E_2} M(E), \tag{71}$$

where we suppress the obvious momentum dependence. Presenting

$$P_E = \int dt P(t) e^{iEt}, \quad M(E) = \int d\tau M(\tau) e^{iE\tau}$$

we have

$$\begin{aligned}
Z_1(t) &= \int dt_1 dt_2 dt_3 dt_4 d\tau \int \frac{dE dE_1 dE_2}{(2\pi)^3} e^{i(E-E_1)t_1 + iE_1 t_2 + i(E-E_2)t_3 + iE_2 t_4 + iE\tau} \\
P_1(t-t_1) P_2(t-t_2) P_3(t_3) P_4(t_4) M(\tau) &= \int_0^t dt_1 \int_0^{t_1} dt_2 P_1(t-t_1) P_2(t-t_1) M(t_1-t_2) P_3(t_2) P_4(t_2), \tag{72}
\end{aligned}$$

where we take into account that both $P(t)$ and $M(t)$ are zero at $t < 0$. Analytically continuing to rapidities we find

$$Z_1(y) = - \int_0^y dy_1 \int_0^{y_1} P_1(y-y_1) P_2(y-y_2) M(y_1-y_2) P_3(y_2) P_4(y_2). \tag{73}$$

So in the end

$$D_{3a} = \theta(y) \int_0^y dy_1 \int_0^{y_1} dy_2 \int \prod_{j=1}^4 \frac{d^2 q'_j}{(2\pi)^2} \frac{d^2 q_j}{(2\pi)^2} 2\pi \delta^2 \left(\sum_{j=1}^4 q'_j - \sum_{j=1}^4 q_j \right)$$

$$P_{12}(y - y_1, q_1) P_{34}(y - y_1, q_4) < q_1, -q_1, -q_4, q_4 | M^{(a)}(y_1 - y_2) | q'_1, -q'_4, -q'_2, q'_4 > P_{13}(y_2, q'_1) P_{24}(y_2, q'_4) \quad (74)$$

and

$$D_{3b} = \theta(y) \int_0^y dy_1 \int_0^{y_1} dy_2 \int \prod_{j=1}^4 \frac{d^2 q'_j}{(2\pi)^2} \frac{d^2 q_j}{(2\pi)^2} 2\pi \delta^2 \left(\sum_{j=1}^4 q'_j - \sum_{j=1}^4 q_j \right)$$

$$P_{12}(y - y_1, q_1) P_{34}(y - y_1, q_4) < q_1, -q_1, -q_4, q_4 | M^{(b)}(y_1 - y_2) | q'_1, -q'_4, -q'_2, q'_4 > P_{12}(y_2, q'_1) P_{34}(y_2, q'_4), \quad (75)$$

where we indicated the numbers of reggeized gluons of which different pomerons are made.

6 The deuteron-deuteron scattering

The total deuteron-deuteron scattering cross-section apart from the contributions studied in the previous sections will include the standard single and double scattering terms (see Appendix 1. Figs. 10 and 14). So the total cross-section is the sum

$$\sigma^{dd} = \sigma^{single} + \sigma^{double} + \sum_{i=1}^3 \sigma^{(i)}. \quad (76)$$

Here the single cross-section is well known

$$\sigma^{single} = \sigma_{pp} + \sigma_{nn} + 2\sigma_{pn}. \quad (77)$$

The double cross-section is (see Appendix 1.)

$$\sigma^{double} = -\frac{1}{2}(\sigma_{pp}\sigma_{nn} + \sigma_{pn}^2) \int d^2 b T_d^2(b), \quad (78)$$

where the transverse density $T(b)$ is expressed in the standard manner via the deuteron wave function:

$$T_d(b) = \int dz |\psi_d(b, z)|^2. \quad (79)$$

Finally the additional cross-sections due to the QCD effects are expressed via D_i , $i = 1, 2, 3$ according to Eq. (4)

$$\sigma^{(i)} = -2D_i N_c^2 \left(\langle \frac{1}{2\pi r^2} \rangle_d \right)^2, \quad (80)$$

where $\langle \dots \rangle_d$ means averaging in the deuteron.

7 Discussion

For high-energy nucleus-nucleus scattering we have calculated the leading terms in the eikonal function for the forward scattering amplitude corresponding to the collision of two scattering centers in the projectile nucleus with two scattering centers in the target nucleus. Apart from the obvious pomeron exchange, these terms include contributions from connected diagrams involving two pomerons from the projectile and two pomerons from the target with all possible interactions in between. We have demonstrated that the result is infrared safe, as one expected. It is remarkable that it involves contributions from intermediate BKP states formed by 4 reggeized gluons.

For the deuteron-deuteron scattering the total cross-section is the sum of the eikonal function plus the double scattering term in Eq. (76). If one takes the pomerons as described by the BFKL equation

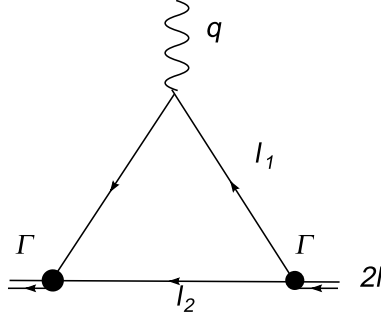


Figure 9: Electromagnetic form factor of the deuteron

then the behaviour of the dd cross-section will roughly correspond to the double pomeron exchange that is $\exp(2\Delta_{BFKL}y)$, where $\Delta_{BFKL} = (\alpha_s N_c / \pi) 4 \ln 2$ is the BFKL intercept. Note that in this case the intermediate BKP state in $\sigma^{(3)}$ will enter at comparatively low energies, so that one cannot use its asymptotical behaviour to find the result. On the other hand description of the total NN cross-section by the single pomeron exchange is obviously unrealistic. The single and double cross-sections in (4) can be calculated using the experimental values of this cross-section. As to the rest, instead of simple BFKL pomerons one may use unitarized expressions corresponding to sums of fan diagrams and found as solutions of the BK equation. The latter do not grow at high energies and so the asymptotical behaviour of the cross-section will be determined by that of the BKP state entering $\sigma^{(3)}$, which grows, although not so fast as the pomeron ($\sim \exp 0.243 \Delta_{BFKL}y$, [14]). As a result the dd cross-sections allow for the direct experimental study of the behaviour of such states, theoretical calculation of which presents serious difficulties.

This is of course true also for collisions of heavy nuclei. But in this case unitarization of the eikonal function will in any case lead to the total cross-section which are more or less geometrical. Additional terms in the eikonal may of course change it considerably but the cross-section will not change at least inside the nucleus where the eikonal remains large. In this case a more interesting problem is the inclusive gluon production in the nucleus-nucleus collisions to which disconnected diagrams do not contribute. This requires cutting our forward scattering amplitude to select the observed intermediate states with due attention to possible cancellation between real and virtual processes (AGK cancellations). This problem will be dealt in future studies.

8 Acknowledgments

This work has been supported by grant RFFI 12-02-00356-a. The author is thankful to J.B.Bartels and G.P.Vacca for their interest in this study and helpful discussions. He also thanks the INFN and Universities of Bologna and Hamburg for hospitality.

9 Appendix 1. Deuteron in the Glauber approach

9.1 Scattering on the deuteron

To formulate the Glauber approach to the collisions with deuteron in the diagrammatic technique we first have to relate the relativistic dnp vertex Γ with the deuteron wave function. To this end we study the electromagnetic form-factor of the deuteron, illustrated in Fig. 9, where vertices Γ are shown with blobs. In the lab. system and at zero momentum transfer it is equal to $2M$ where $M = 2m - \epsilon$ is the deuteron mass. So we get the normalization condition

$$\int \frac{d^4 l_2}{((2\pi)^4 i)} \frac{2l_{10} \Gamma^2(l_2)}{(m^2 - l_2^2 - i0)(m^2 - l_1^2 - i0)^2} = 2M. \quad (81)$$

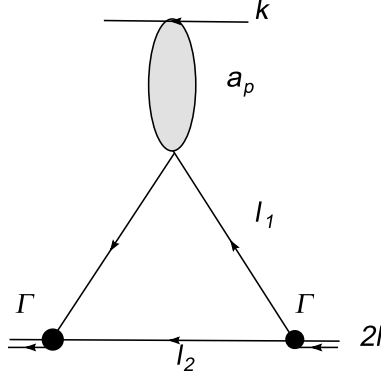


Figure 10: Scattering on the deuteron in the impulse approximation

Here $l_1 + l_2 = 2l$ and $4l^2 = M^2$. We neglect spins and consider all particles as scalar for simplicity. We have $l_0 = m - \epsilon/2$, and $\mathbf{l} = 0$, so that putting $l_2 = l + \lambda$ we find

$$m^2 - l_2^2 = -2m\lambda_0 - \lambda_\perp^2, \quad m^2 - l_1^2 = 2m\lambda_0 - \lambda_\perp^2,$$

where we used the orders of magnitude $\lambda_0 \sim \epsilon$, $|\lambda_\perp| \sim \sqrt{m\epsilon}$. Integration over λ_0 transforms (81) into

$$\int \frac{d^3 l_2}{(2\pi)^3} \frac{\Gamma^2(\mathbf{l}_2)}{8m(m\epsilon + \mathbf{l}_2^2)^2} = 2. \quad (82)$$

Comparing with the standard normalization of the deuteron wave function $\psi_d(\mathbf{l})$ we find the desired relation

$$\psi_d(\mathbf{l}) = \frac{\Gamma(\mathbf{l})}{4(2\pi)^{3/2}\sqrt{m}(m\epsilon + \mathbf{l}^2)}, \quad (83)$$

which allows to relate the relativistic $d p n$ vertex with the deuteron wave function in the momentum space.

In the impulse approximation, Fig. 10, with the spectator neutron the corresponding amplitude is given by

$$\mathcal{A}^{imp} = a \int \frac{d^4 l_2}{(2\pi)^4 i} \frac{\Gamma^2(\mathbf{l}_2)}{(m^2 - l_2^2 - i0)(m^2 - l_1^2 - i0)^2}, \quad (84)$$

where a is the forward scattering amplitude on the proton. Using (81) we find that the integral is equal to 2 and we get $\mathcal{A}^{imp} = 2a$. But the relativistic flux on the deuteron is twice that on the proton, so that we get $\sigma_d = \sigma_p + \sigma_n$, where the second term takes into account the diagram of Fig. 10 with the spectator proton.

Now consider double scattering on the deuteron illustrated in Fig. 11. The amplitude is given by

$$\mathcal{A} = \int \frac{d^4 l_2}{(2\pi)^4 i} \frac{d^4 l'_2}{(2\pi)^4 i} H(l_{2z} - l'_{2z}) \frac{\Gamma(\mathbf{l}_2)}{(m^2 - l_1^2 - i0)(m^2 - l_2^2 - i0)} \frac{\Gamma(\mathbf{l}'_2)}{(m^2 - l_1'^2 - i0)(m^2 - l_2'^2 - i0)}, \quad (85)$$

where H is the high-energy part and it is taken into account that it can only depend on the z -component of the transferred momentum, since it is the only of the spatial components which enters multiplied by the high projectile momentum.

Integrations over the zero components of the nuclear momenta factorize and we get

$$\mathcal{A} = \int \frac{d^3 l_2 d^3 l'_2}{(2\pi)^3} H(l_{2z} - l'_{2z}) \frac{\Gamma(\mathbf{l}_2)}{4m(m\epsilon + \mathbf{l}_2^2)} \frac{\Gamma(\mathbf{l}'_2)}{4m(m\epsilon + \mathbf{l}'_2^2)}, \quad (86)$$

or using (83)

$$\mathcal{A} = \frac{1}{m} \int \frac{d^3 l_2 d^3 l'_2}{(2\pi)^3} H(l_{2z} - l'_{2z}) \psi_d(\mathbf{l}_2) \psi_d(\mathbf{l}'_2). \quad (87)$$

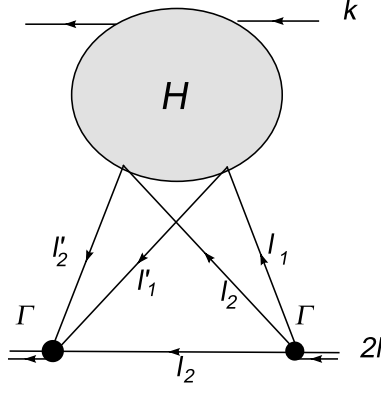


Figure 11: Double scattering on the deuteron

Integrations over the transverse components are done immediately to convert the wave functions into those with the transverse coordinates zero:

$$\mathcal{A} = \frac{1}{m} \int \frac{dl_{2z} dl'_{2z}}{2\pi} H(l_{2z} - l'_{2z}) \psi_d(r_\perp = 0, l_{2z}) \psi_d(r_\perp = 0, l'_{2z}). \quad (88)$$

Transforming completely to the coordinate space we find

$$\mathcal{A} = \frac{1}{m} \int \frac{dl_{2z}}{2\pi} \frac{dq_z}{2\pi} dz dz' H(q_z) \psi_d(r_\perp = 0, z) \psi_d(r_\perp = 0, z') e^{il_{2z}(z-z') - iq_z z'}, \quad (89)$$

where we introduced the z -component of the transferred momentum putting $l'_z = l_z + q_z$. Integration over l_{2z} gives our final expression

$$\mathcal{A} = \frac{1}{m} \int \frac{dq_z}{2\pi} dz H(q_z) |\psi_d(r_\perp = 0, z)|^2 e^{-iq_z z}. \quad (90)$$

The Glauber approximation follows if $H(q_z)$ has a singularity at $q_z = 0$. Typically

$$\text{Im } H(q_z) = -\hat{D}(2\pi)\delta(2kq) = -\hat{D}\frac{\pi}{k_0}\delta(q_z). \quad (91)$$

Here we use $q_0 \ll |q_z|$ and $k_0 = k_z > 0$. In this case we get the Glauber approximation for the double scattering amplitude

$$\text{Im } \mathcal{A} = -\frac{1}{s} \hat{D} \int dz |\psi_d(r_\perp = 0, z)|^2 = -\frac{1}{s} \hat{D} < \frac{1}{2\pi r^2} >_d. \quad (92)$$

where $< \dots >_d$ means the average in the deuteron. The cross-section is

$$\sigma_d = -\frac{1}{2s^2} \hat{D} < \frac{1}{2\pi r^2} >_d. \quad (93)$$

To see how this formula works consider the simplest case of the double scattering corresponding to double elastic collision shown in Fig. 12. In this case

$$H(q_z) = ia_p a_n \left(\frac{-i}{m_2 - (k + q_z)^2 - i0} + \frac{-i}{m_2 - (k - q_z)^2 - i0} \right) = ia_p a_n 2\pi \delta(2k_0 q_z), \quad (94)$$

so that $\hat{D} = -a_p a_n$. Using (92) we find

$$\text{Im } \mathcal{A} = a_p a_n \frac{1}{s} < \frac{1}{2\pi r^2} >_d = -s \sigma_p \sigma_n < \frac{1}{2\pi r^2} >_d. \quad (95)$$

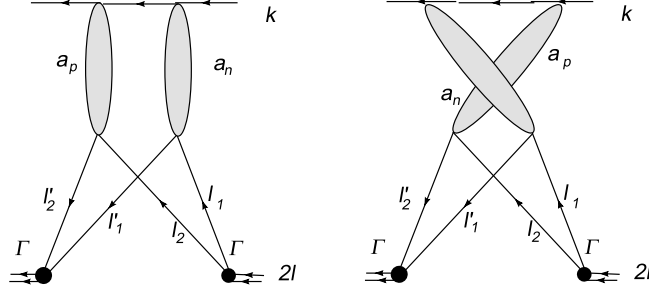


Figure 12: Double elastic collision on the deuteron

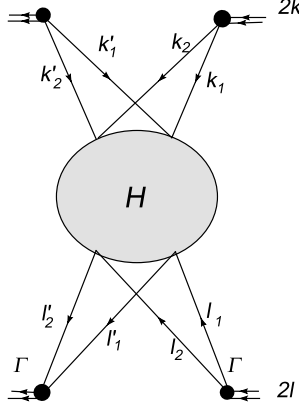


Figure 13: Double scattering in deuteron-deuteron collisions

From this dividing by $2s$ and doubling to take into account the crossed diagram find the double cross-section

$$\sigma^{double} = -\sigma_p \sigma_n < \frac{1}{2\pi r^2} >_d. \quad (96)$$

For the nuclear target instead of (93) we have at fixed impact parameter b

$$\sigma_A(b) = -\frac{1}{2s^2} \hat{D} T_A^2(b) \quad (97)$$

and for double elastic collisions instead of (96)

$$\sigma_A(b) = -\frac{1}{2} A(A-1) \sigma_N^2 T_A^2(b). \quad (98)$$

To conclude we note that H and F are both Lorentz invariant. So (91) can be used to find F in any system.

9.2 Double scattering in d-d collisions

Now consider the case when two deuterons collide at high energies and each one experiences double collision, illustrated in Fig. 13. Our treatment is to consider subsequently the two systems in which the deuteron is well understandable, the rest systems of the target and projectile deuterons.

We start from the rest system of the target deuteron. We use Eq. (92) and write

$$\text{Im } \mathcal{A} = -\frac{1}{s} \hat{D}_1 < \frac{1}{2\pi r^2} >_d, \quad (99)$$

where it is assumed that $\text{Im } H_1 = -\hat{D}_1 2\pi \delta(2kq)$ and we include into H_1 all the rest part of the diagram in Fig. 13 including the coupling to the projectile nucleons.

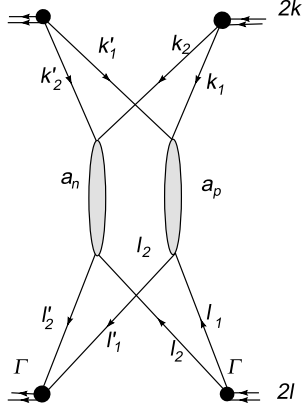


Figure 14: Double elastic collision in deuteron-deuteron scattering

Now we boost the system into the rest one for the projectile. In this system we can repeat our treatment of the coupling to the two nucleons. If $\hat{D}_1 = \hat{D}2\pi\delta(2l\kappa)$ where κ is the momentum transferred from the projectile, integration over the nucleon momenta will give the same factor $(1/s) < 1/2\pi r^2 >_d$ and we shall get

$$\text{Im } \mathcal{A} = -\left(\frac{1}{s}\right)^2 \hat{D} < \frac{1}{2\pi r^2} >_d^2. \quad (100)$$

Note that we have

$$\text{Im } H = -\hat{D}(2\pi)^2\delta(2(l\kappa))\delta(2(kq)). \quad (101)$$

This means that (100) is symmetric in projectile and target, as expected. From (100) we immediately get the cross-section (4) taking in to account the definition of D , Eq. (2)

Special attention is to be given for the case when the high-energy part H is disconnected, shown in Fig. 14. Then H contains a δ function corresponding to conservation laws for the two connected parts and is given by

$$H = i(a_{pp}a_{nn} + a_{pn}^2)(2\pi)^4\delta^4(k_1 + l_1 - k'_1 - l'_1). \quad (102)$$

Factor i combines $(-i)$ from the definition of \mathcal{A} and i^2 from the two NN amplitudes. Note that

$$\begin{aligned} (2\pi)^4\delta^4(k_1 + l_1 - k'_1 - l'_1) &= (2\pi)^4\delta(\kappa_+ + q_+)\delta(\kappa_- q_-)\delta^2(k_{1\perp} + l_{1\perp} - k'_{1\perp} - l'_{1\perp}) \\ &= 2s(2\pi)^2\delta(2(l\kappa))\delta(2(kq)) \int d^2b e^{ib(k_{1\perp} + l_{1\perp} - k'_{1\perp} - l'_{1\perp})}. \end{aligned}$$

As we see, integrations over the transverse coordinates of the nucleons in the projectile and target become interdependent. Under the sign of integration over b we include the exponentials depending on the transverse momenta of the projectile and target in the corresponding integrals to obtain in (88) $\psi_d(b, l_{2z})\psi_d(b, l'_{2z})$ instead of $\psi_d(r_\perp = 0, l_{2z})\psi_d(r_\perp = 0, l'_{2z})$ and similarly for the projectile. All subsequent calculations remain unchanged and in the end we obtain in (92)

$$\int dz |\psi_d(b, z)|^2 \equiv T_d(b) \quad (103)$$

instead of

$$\int dz |\psi_d(r_\perp = 0, z)|^2 = < \frac{1}{2\pi r^2} >_d.$$

So the net result of the connection between the transferred transverse momenta is to substitute $< 1/2\pi r^2 >_d \rightarrow T_d(b)$ both in the projectile and target and then integrate over b . The rest factors from H give $\hat{D} = 2sa_p a_n$ and from (100) we conclude

$$\text{Im } \mathcal{A} = \frac{2}{s}(a_{pp}a_{nn} + a_{pn}^2) \int d^2b T_d^2(b) \quad (104)$$

Dividing by $4s$ we find the cross-section

$$\sigma_{dd} = -\frac{1}{2}(\sigma_{pp}\sigma_{nn} + \sigma_{pn}^2) \int d^2b T_d^2(b) \quad (105)$$

which looks very much like the standard Glauber formula.

For the collision of two heavy nuclei instead of Eq. (105) we shall get at fixed b

$$\sigma_{AB}(b) = -\frac{1}{4}A(A-1)B(B-1)\sigma_N^2 \left(\int d^2b_A T_A(b_A) T_B(b-b_A) \right)^2. \quad (106)$$

10 Appendix 2. Colour factors

The explicit expressions for the colour wave functions of the projectile and target in which pairs (12),(34) and (13),(24) respectively form colour singlets are:

$$|(12)(34)\rangle = \frac{1}{N_c^2} \delta_{a_1 a_2} \delta_{a_3 a_4}, \quad |(13)(24)\rangle = \frac{1}{N_c^2} \delta_{a_1 a_3} \delta_{a_2 a_4}. \quad (107)$$

Here we neglect terms of the relative order $1/N_c^2$. Their scalar product is

$$\langle (13)(24) | (12)(34) \rangle = \frac{1}{N_c^4} \delta_{a_1 a_3} \delta_{a_2 a_4} \delta_{a_1 a_2} \delta_{a_3 a_4} = \frac{1}{N_c^2}, \quad (108)$$

which is the overall damping factor accompanying all diagrams with the redistribution of colour like Fig. 2.

We denote $C_{ij} = -(T_i T_j)$. For interactions connecting vacuum pairs either in the projectile or in the target $C_{ij} = N_c$

$$\langle (13)(24) | C_{ij} | (12)(34) \rangle = N_c \langle (13)(24) | (12)(34) \rangle = \frac{1}{N_c}, \quad (ij) = (12), (34), (13), (24) \quad (109)$$

For the remaining two interactions we find

$$\langle (13)(24) | C_{14} | (12)(34) \rangle = \frac{1}{N_c^4} \delta_{a'_1 a'_3} \delta_{a'_2 a'_4} \delta_{a_1 a_2} \delta_{a_3 a_4} \delta_{a'_2 a_2} \delta_{a'_3 a_3} f^{a'_1 a_1 c} f^{a'_4 a_4 c} = \frac{1}{N_c^4} f^{a_3 a_1 c} f^{a_1 a_3 c} = -\frac{1}{N_c}. \quad (110)$$

Interchange $(1 \leftrightarrow 2), (3 \leftrightarrow 4)$ gives

$$\langle (13)(24) | C_{23} | (12)(34) \rangle = -\frac{1}{N_c}. \quad (111)$$

So effectively for these interactions $C_{ij} = -N_c$

Apart from states $|(12)(34)\rangle$ and $|(13)(24)\rangle$ in the diagrams we encounter six BKP states with different ordering of the 4 gluons:

$$|1234\rangle, |1243\rangle, |1324\rangle, |1342\rangle, |1423\rangle, |1432\rangle.$$

In the high colour limit their explicit form is

$$|1234\rangle = \frac{1}{2N_c^2} h^{a_1 a_2 c} h^{a_3 a_4 c}, \quad (112)$$

where $h^{abc} = d^{abc} + i f^{abc}$ with the properties

$$[h^{abc}]^* = h^{bac}, \quad \sum_{cd} [h^{acd}]^* h^{bcd} = \delta_{ab} 2N_c \left(1 - \frac{2}{N_c^2}\right), \quad \sum_{cd} h^{acd} h_{bcd} = -\delta_{ab} \frac{4}{N_c} \quad (113)$$

The states $|ijkl\rangle$ are cyclic symmetric in $(ijkl)$.

Their scalar products with the projectile and target states are

$$\langle (12)(34)|1234 \rangle = \frac{1}{N_c^4} \delta_{a_1 a_2} \delta_{a_3 a_4} h_{a_1 a_2 c} h_{a_3 a_4 c} = 0. \quad (114)$$

$$\langle (13)(24)|1234 \rangle = \frac{1}{N_c^4} \delta_{a_1 a_3} \delta_{a_2 a_4} h_{a_1 a_2 c} h_{a_3 a_4 c} = \frac{1}{N_c^4} h^{a_1 a_2 c} h^{a_1 a_4 c} = -2 \frac{1}{N_c^3}. \quad (115)$$

Generally if (12) or (34) are neighbors in (ijkl) then states $|(12)(kl) \rangle$ and $|ijkl \rangle$ are orthogonal. If they are not the scalar product is the same as in (115).

We also need matrix elements of colour matrices C_{ij} between projectile (target) states and BKP states. Obviously we need only C_{ij} which do not connect vacuum pairs in the projectile (target), namely for $(ij) = (13), (14), (23), (24)$. Then we find that for $(klmn) = ((1234), (2134), (2143)$ and (1423)

$$\langle (12)(34)|C_{ij}|klmn \rangle = \pm \frac{1}{2}, \quad (116)$$

where the sign plus is to be taken when (ij) are neighbours in $(klmn)$ and the sign minus when they are not. Acting on the rest two states $|1324 \rangle$ and $|1423 \rangle$. all matrices C_{13}, C_{24}, C_{14} and C_{23} give $N_c/2$ since neighbour gluons are in the gluon colour state and the matrix elements become damped by $1/N_c^2$. E.g.

$$\langle (12)(34)|C_{13}|1423 \rangle = \frac{N_c}{2} \langle (12)(34)|1423 \rangle = -\frac{1}{N_c^2}. \quad (117)$$

(Note that the correct derivation of (116) and 117) in some cases requires taking into account subdominant terms in (112))

As a result the matrix elements of C_{13} are

$$\begin{aligned} \langle (12)(34)|C_{13}|1234 \rangle &= \langle (12)(34)|C_{13}|2143 \rangle = -\frac{1}{2}, \\ \langle (12)(34)|C_{13}|2134 \rangle &= \langle (12)(34)|C_{13}|1243 \rangle = \frac{1}{2}, \\ \langle (12)(34)|C_{13}|1324 \rangle &= \langle (12)(34)|C_{13}|1423 \rangle = 0, \end{aligned}$$

which implies

$$\langle (12)(34)|C_{13} = -\frac{1}{2} \langle 1234| - \frac{1}{2} \langle 2143| + \frac{1}{2} \langle 2134| + \frac{1}{2} \langle 1243|. \quad (118)$$

Note that the summed probabilities correctly give unity.

Similarly

$$\begin{aligned} \langle (12)(34)|C_{24} &= -\frac{1}{2} \langle 1234| - \frac{1}{2} \langle 2143| + \frac{1}{2} \langle 2134| + \frac{1}{2} \langle 1243|, \\ \langle (12)(34)|C_{23} &= -\frac{1}{2} \langle 2134| - \frac{1}{2} \langle 1243| + \frac{1}{2} \langle 1234| + \frac{1}{2} \langle 2143|, \end{aligned}$$

and

$$\langle (12)(34)|C_{14} = -\frac{1}{2} \langle 2134| - \frac{1}{2} \langle 1243| + \frac{1}{2} \langle 1234| + \frac{1}{2} \langle 2143|.$$

Interchanging $(2 \leftrightarrow 3)$ we get

$$\begin{aligned} C_{12}|(13)(24) \rangle &= -\frac{1}{2}|1324 \rangle - \frac{1}{2}|3142 \rangle + \frac{1}{2}|3124 \rangle + \frac{1}{2}|1342 \rangle, \\ C_{34}|(13)(24) \rangle &= -\frac{1}{2}|1324 \rangle - \frac{1}{2}|3142 \rangle + \frac{1}{2}|3124 \rangle + \frac{1}{2}|1342 \rangle, \\ C_{23}|(13)(24) \rangle &= -\frac{1}{2}|3124 \rangle - \frac{1}{2}|1342 \rangle + \frac{1}{2}|1324 \rangle + \frac{1}{2}|3142 \rangle, \end{aligned}$$

Table 1: Matrix elements of the product C_{ij} (lines) by C_{kl} (columns) between states $< (12)(34)|$ and $|(13)(24) >$

	(12)	(34)	(23)	(14)
(13)	1/2	0	-1/2	-1/2
(24)	0	-1/2	0	0
(23)	-1/2	0	1/2	1/2
(14)	-1/2	0	1/2	1/2

$$C_{14}|(13)(24) > = -\frac{1}{2}|1324 > -\frac{1}{2}|3142 > +\frac{1}{2}|3124 > +\frac{1}{2}|1342 > .$$

These relations allow to study matrix elements of the product of two matrices $C_{ij}C_{kl}$ between the projectile and target states. They are shown in Table 1. with lines (ij) and columns (kl)

From these results we can find the probability to find a particular BKP state between the projectile and target. States $|1234 >$ and $|1324 >$ do not appear and we find the contribution from the double interaction $V_{ij}V_{kl}$ where $V_{ij} = -C_{ij}g^2v_{ij}$

$$\frac{1}{4} < (12)(34)| \left(v_{13} + v_{24} - v_{23} - v_{14} \right) \left(|1243 > < 1243| + |1342 > < 1342| \right) \left(v_{12} + v_{34} - v_{23} - v_{14} \right) |(13)(24) > . \quad (119)$$

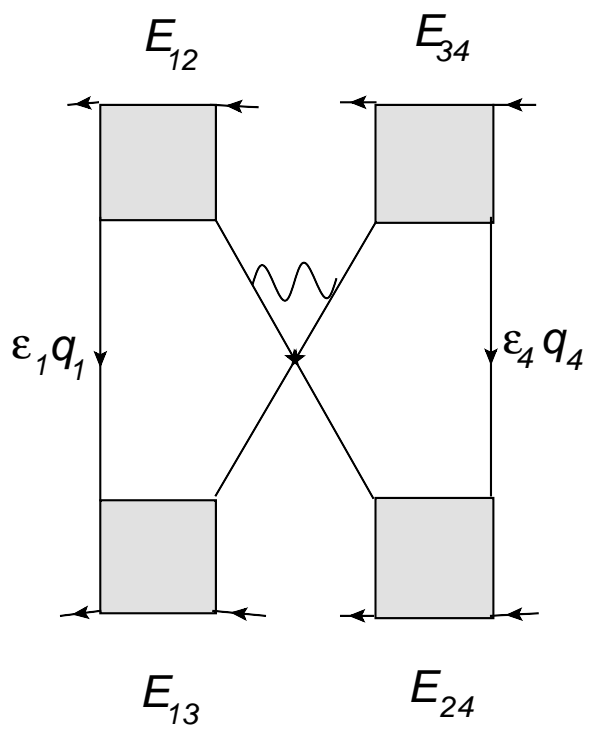
We are also interested in the matrix elements of products of two matrices $C_{ij}C_{kl}$ between projectile and target states without redistribution of color, that is between states $< (12)(34)|$ and $|(12)(34) >$. In particular we shall be interested in separate contribution from BKP states. In this case four different BKP states appear between the projectile and target $|1234 >$, $|1432 >$, $|1342 >$ and $|1243 >$ with equal probability and, similar to (119) we find the probabilities

$$\frac{1}{4} < (12)(34)| \left(v_{13} + v_{24} - v_{23} - v_{14} \right) \left(|1234 > < 1234| + |1243 > < 1243| + |1432 > < 1432| + |1342 > < 1342| \right) \left(v_{13} + v_{24} - v_{23} - v_{14} \right) |(13)(24) > . \quad (120)$$

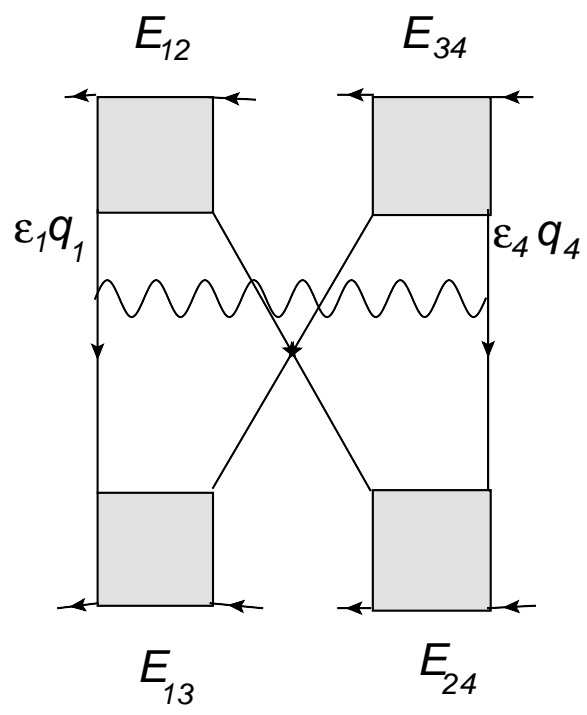
References

- [1] A.Krasnitz, R.Venugopalan, Phys. Rev.Lett.**84** (2000) 4309; **86** (2001) 1717
- [2] A.Krasnitz, Y.Nara, R.Venugopalan, Phys. Rev. Lett.**87** (2001) 192302; Nucl. Phys. **A 727** (2003) 127; Phys. Lett. **B 554** (2003) 21.
- [3] T.Lappi, Phys. Rev. **C 67** (2003) 054903; **C 70** (2004) 054905; Phys. Lett. **B 643** (2006) 11.
- [4] Yu. V. Kovchegov, Nucl. Phys. **A 692** (2001) 567.
- [5] I.Balitski, Phys. Rev. **D 72** (2005) 074027.
- [6] K.Dusling, F.Gelis, T. Lappi, R.Venugopalan, Nucl. Phys. **A 836** (2010) 159.
- [7] L.N.Lipatov, in: "Perturbative QCD" p.411, ed. A.H.Mueller, World Scientific, Singapore, 1989,
- [8] I.Balitski, Nucl. Phys. **B 463** 99.
- [9] Yu. V. Kovchegov. Phys. Rev. **D 60** (1999) 034008
- [10] J.Bartels, Nucl. Phys. **B 175** (1980) 365.

- [11] J.Kwiecinski, M.Praszalowicz, Phys. Lett. **B 94** (1980) 413.
- [12] A.Dumitru, J. Jalilian-Marian, Phys. Rev. **D 81** (2010) 094015.
- [13] M.A.Braun, Eur. Phys. J. **C 6** (1999) 321.
- [14] G.P.Korchemsky, J.Kotansky and A.N. Manashov, Phys. Rev. Lett. **88** (2002) 122002.



a



b